Imaging of laser-induced plasma species

M. Bator, C. W. Schneider, T. Lippert
Paul Scherrer Institute, Department General Energy, Villigen PSI, Switzerland (May 2013)

Application Note

1 Introduction

Multiferroics, materials comprising two or more ferroic properties, such as ferromagnetism, ferroelectricity or ferroelasticity in the same phase, are very promising systems for future applications in computing or sensing. These materials would allow to design new digital storage devices thereby combining the advantages of long lived magnetic storage with easy accessibility and robustness of electronic storage technology. Still, materials combing both properties to be useful for applications are scarce. To better adapt multiferroic properties, thin film growth introduces new parameters such as strain, allowing the tuning of materials properties. For a targeted growth control optical emission spectroscopy and time resolved imaging is utilized to investigate the plasma during the growth by pulsed laser deposition.

2 Materials and Methods

Pulsed laser deposition (PLD) is a very powerful tool to evaporate in vacuum or in a background atmosphere a materials, either metal or ceramic, thereby creating a plasma. The species from this plasma cloud are condensing on a substrate and in that way forming a film. The material $LuMnO_3$ with an orthorhombic structure is a promising multiferroic, however the orthorhombic structure is metastable and therefore not easy to synthesize as bulk to study its electrical and magnetic properties. The preparation as a thin film is one way to obtain high quality material with the correct crystalline structure but the preparation as a thin film is not easy to accomplish. In order to investigate the PLD deposition of $LuMnO_3$, in particular the properties of laser induced Lu plasma species from from three different Lu-containing targets were studied: A metal Lu disc target, a ceramic Lu_2O_3 disc target, and a cylindrical ceramic target of hexagonal-$LuMnO_3$. For the ablation of these targets, a KrF excimer laser (λ = 248 nm) was used at a repetition rate of 8 Hz with a laser fluence of ~3.5 J/cm^2. A 9 x 9 mm^2 mask was imaged onto the target resulting in approx. 1.7 mm^2 spot size of the laser beam. The background pressure was varied from vacuum (1 x 10^{-8} mbar) to 1.5 x 10^{-3} and 5 x 10^{-2} mbar using N_2O and O_2 background gases.

To study the plasma properties, plasma imaging was performed using an Andor Solis software and a USB iStar camera – DH334T-18F-03 equipped with an acousto-optical tuneable filter (AOTF, Brimrose VA210 .40 .65 H) for the wavelength range of 400 - 650 nm. The wavelength resolution is ~0.8 nm for the short wavelengths, and up to 2.1 nm around 650 nm. The settings for gating, frame repetition and delay times are mentioned in the respective parts of the discussion. To image the entire plasma (4 cm) including the target and the mass spectrometer nozzle onto the CCD a Nikkor 28 - 300 mm lens was used at a distance of 550 mm to the plasma set to ~200 mm focal length. These time and space resolved optical emission studies where complemented by plasma mass spectroscopy measurements to determine the plasma composition and the respective kinetic energy of these species. Both, the mass spectrometry and the plasma imaging were triggered from the same photodiode placed in the beam path and used simultaneously to assure consistency of the results as illustrated in Fig. 1.

The emitted plasma radiation was measured as a function of time, space and wavelength. Changes in relative intensities between Lu and LuO lines over time show a distinct behaviour when comparing vacuum conditions with an oxidizing background gas. While the initial expansion of plasma species for all background conditions is similar, the behaviour changes at later times when the interaction between species from the target and the background become dominant. In an oxidizing background gas the relative intensities increase favouring the oxidized species which agrees well with observations from mass spectrometry.

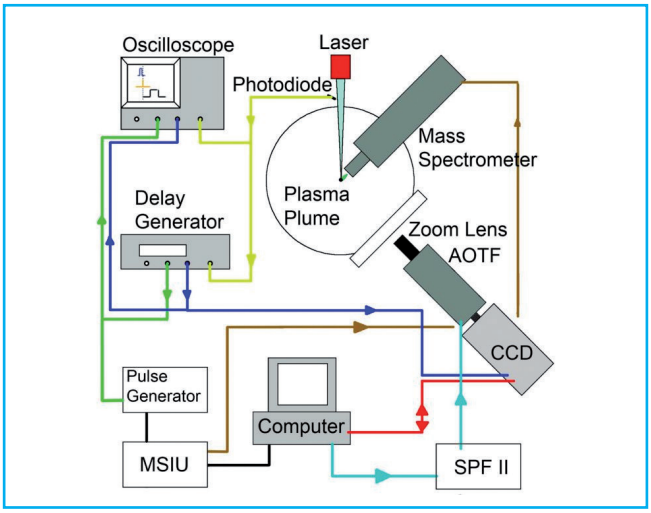

Figure 1: The top view of the UHV chamber is fitted with a target in the centre. The pulsed laser beam generates a plasma plume that is directed towards the mass spectrometer. Perpendicular to the plasma expansion a window allows the investigation of the plasma by optical methods. A lens system images the plasma through the acoustooptical tuneable filter onto a high-speed CCD.

Imaging of laser-induced plasma species

M. Bator, C. W. Schneider, T. Lippert
Paul Scherrer Institute, Department General Energy, Villigen PSI, Switzerland (May 2013)

Application Note

3 Plasma imaging

In plasma imaging, the entire plasma is pictured with a specific filter selecting ideally a single wavelength with a gate width of 10 µs to capture the integrated intensity for the time the plasma exists. In Fig. 2 the emissions from the Lu target at 499 nm (a) (Lu I) and 518.5 nm (b) (LuO) are shown and compared to an optical photograph (c). From these measurements, the integrated spatial expansion of these species can be studied. Whereas excited Lu species seem to reach the mass spectrometer respective substrate position, the intensity for excited LuO is severely diminished. This is confirmed by the mass spectrometry measurements where the number of LuO arriving at the substrate position is approx. 100 times smaller than Lu.

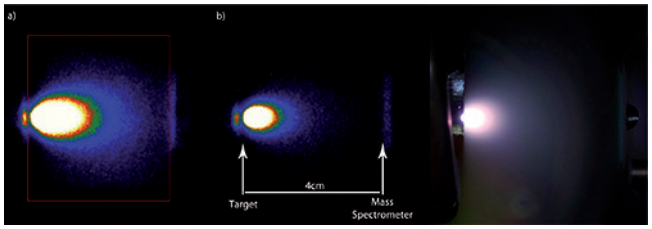

Figure 2: a) Lu I emission at 499 nm. The red square shows the area over which the intensities were integrated. b) Emission from a LuO line at 518.5 nm.c) Photograph of the plasma. All pictures are taken at a fluence of 3.5 J/cm² in vacuum.

Introducing N_2O as a reactive background gas to enhance the creation of metal oxide species needed to form orthorhombic $LuMnO_3$, we observe as a function of the background pressure an increase in the number of metal oxide species due to chemical reactions taking place in the plasma cloud. At a pressure of $5x10^{-2}$ mbar N_2O, the distribution of excited Lu and LuO species in the plasma is very different compared to the ablation in vacuum. In Fig. 3a) the distribution of LuI (red) is shown with a fall-off of the excitation intensity already halfway between the target and the mass spectrometer position. Contrary to the decrease of the excited Lu species the excitation from LuO becomes stronger with increasing distance from the target for the following reason. Due to a much reduced mean free path of these plasma species at this pressure the number of collisions increases and hence the chemical activity thereby creating more LuO species further away from the target. These collisions also contribute to a re-excitation of LuO and enhance the lifetime of these excited species which can be observed as a half-moon shaped distribution around the area covered by LuI (Fig. 3b)). If comparing the extend of the LuO cloud to the optical image in Fig. 3c, both areas coincides reasonably well.

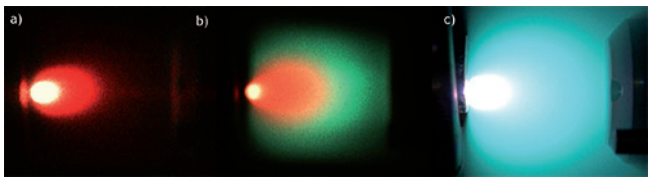

Figure 3: Overlays of false-coloured Lu I (red) and LuO (blue/green) in a) vacuum and b) $5x10^{-2}$ mbar N_2O (factor of 10 in intensity compared to a)). c) A photograph of the plasma at $5x10^{-2}$ mbar N_2O.

Additional information about the process inside the plasma can be gained by time-resolved measurements. Therefore, the gate is reduced to 50 ns, each frame consists of 50 single shot measurements and the delay time increase between the 30 frames is 90 ns. In Fig. 4, a selection of frames taken for three different background conditions (corresponding to the three blocks, each containing pictures for Lu I (top) and LuO (bottom)) is shown. The intensity scale is constant for the two lower pressures, with ten times larger scale for the highest pressure. The bright horizontal line for the first pictures is due to internal reflections of the lens (lens-flare effect for bright point light sources). The behaviour changes dramatically going from vacuum to 1.5×10^{-3} and then to 5×10^{-2} mbar. In vacuum the intensity of the Lu I emission is stronger than the LuO intensity during the whole ablation process. The LuO emission becomes similar in intensity for the intermediate pressure and is even stronger than the Lu I emission very late in the process. A significant change happens for the highest pressure where the LuO intensity surpasses the Lu I emission after ~1000 ns. The difference further increases for later stages of the plasma expansion process. In particular for later times the plasma species move with a common speed in a so-called shockwave where most of the interaction with the background, and therefore the oxidation takes place.

Integrating the intensities from Fig. 4 shows that from vacuum to the intermediate pressure, an increase of the intensities for both Lu I and LuO is observed with a small increase in the LuO/Lu I ratios. At the highest pressure a strong increase of the LuO intensities is observed after ~400 ns with a maximum around 1200 –1300 ns at which the plasma reaches the mass

Imaging of laser-induced plasma species

M. Bator, C. W. Schneider, T. Lippert
Paul Scherrer Institute, Department General Energy, Villigen PSI, Switzerland (May 2013)

Application Note

spectrometer, agreeing well with the observations of species distribution in the plasma. At the highest pressure, the oxidation at the shockwave becomes the dominant factor and leads to a strong oxidation of the metal Lu species to LuO and higher oxides, as confirmed by mass spectrometry.

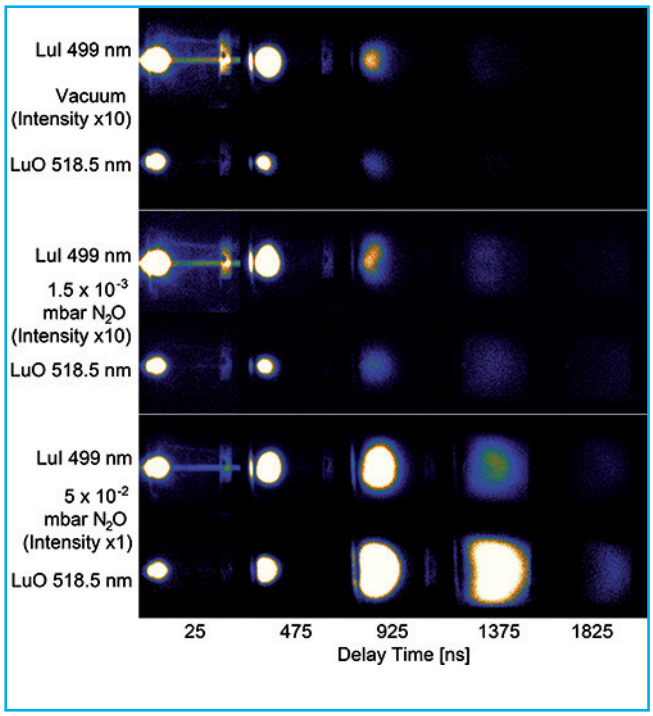

Figure 4: Plasma images for Lu I (top row of each block) and LuO (bottom row of each block) at different delay times for three different background conditions: a) vacuum, b) 1.5 x 10^{-3} mbar N_2O, and c) 5 x 10^{-2} mbar N_2O. All measurements performed on the Lu target.

Contact
PD Dr. Christof W. Schneider
Senior Scientist
Paul Scherrer Institute
OFLB/U111
5232 Villigen – PSI
Switzerland

phone: +41 (0)56 310 4122
fax: +41 (0)56 310 2688
e-mail: christof.schneider@psi.ch
http://www.psi.ch/materials/about-materials-group